Modeling of a Shape Memory Material based Folding Structure: towards Self-reconfigurable Origami Robots

Umar S. Malik[a], Kejun Hu[a], Morvan Ouisse[a], and Kanty Rabenorosoa[a]

[a]FEMTO-ST Institute, Université Bourgogne Franche-Comté, CNRS, 32 Avenue l'Observatoire, Besançon, France

ABSTRACT

Origami robots are becoming very popular due to their excellent morphing abilities and ease of manufacturing. The use of Shape Memory Materials (SMM) for actuation in such structures have not only been proven to make them robust and adaptable to different conditions but also to provide special capabilities. Particularly, Shape Memory Alloy (SMA) actuators have been used for the self-folding/deployment of smart structures. This study presents a Finite Element Analysis (FEA) based thermomechanical model which couples a torsional SMA actuator with a rigid host structure using Shape Memory Polymer (SMP). A specific technique is used for the solution convergence of a complex nonlinear model. After folding the structure to an initial rotation, the influence of SMP stiffness on a Shape Memory Effect (SME) activated rotational motion is investigated. Additionally, the influence of SMP on the global rotational stiffness of such inherently soft structures is studied. The model serves as a starting point for a FEA-based design approach of SMM-equipped singular origami structures and can be topologically optimized for specific applications.

Keywords: Shape Memory Alloy, Shape Memory Polymer, Origami robots, Torsional Actuator, Shape Changing, Shape Blocking, Finite Element Analysis

1. INTRODUCTION

Origami is the art of paper folding which dates back to the 16th century and is known to be discovered by the Japanese. Traditionally, origami involves the manual manipulation of paper to transform it into complex 3D shapes. There are many avenues where origami can be used[?]. For example, its excellent morphing abilities makes it an ideal candidate in space,[?] biomedical,[?] or acoustic[?] applications.

Integration of origami in the field of robotics is a relatively new and fascinating field where 'Origami Robots' are designed to have extraordinary capabilities[?]. An origami robot is a moving device whose morphology and functions are based on self deployment/folding. Ref. **?** used the waterbomb origami structure to build deformable wheels of a mobile robot. Robogami is a robot developed by ref. **?** demonstrating multi DOF motion using (soft) sheet SMA actuators.

In recent times, the introduction of smart materials in origami robots has enhanced their performance to new levels[?]. The mechanical properties of smart materials can vary with a physical property like temperature and manipulating it can impart fascinating behaviours in the structure. For example, figure 1 (adapted from ref. **?**) shows a comparison of the elastic modulus vs. temperature for SMA, SMP and conventional metallic materials. Metallic materials have a nearly constant elastic modulus, thus having similar properties at all temperatures, however, SMA exhibits properties such as Shape Memory Effect (SME) and Pseudo Elasticity (PE). Similarly, based on the temperature-dependent elastic modulus, SMP becomes soft or rigid, thus acquiring the ability of blocking or enabling the structure. Ref. **?** demonstrated the self-folding capability of origami using shape memory polymers. Owing to a hybrid approach (using torsional actuators) dynamic shape changing and (utilizing

Further author information:
U.S.Malik: E-mail: umar_saeed.malik@edu.univ-fcomte.fr
K.Hu: E-mail: kejun.hu@femto-st.fr
M.Ouisse: E-mail: morvan.ouisse@femto-st.fr
K.Rabenorosoa: E-mail: rkanty@femto-st.fr

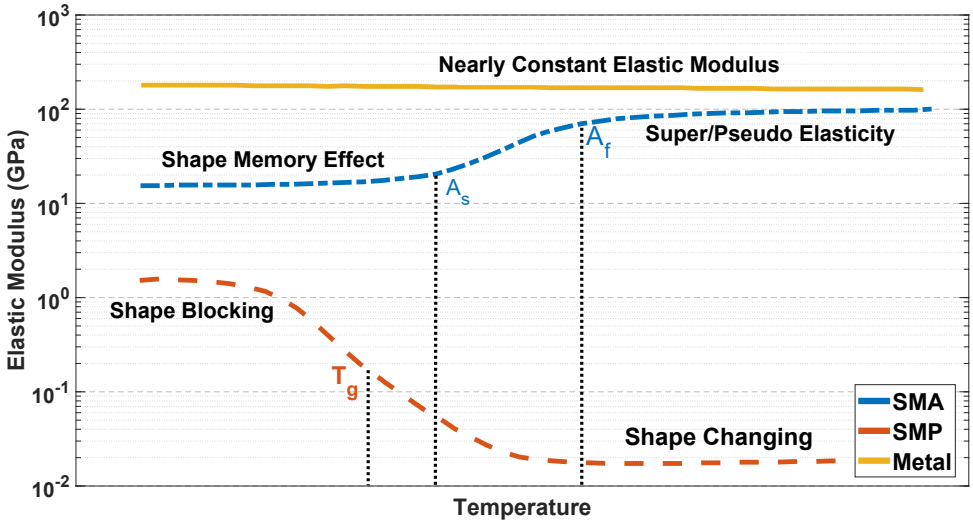

Figure 1: Variation of elastic modulus with temperature for different classes of materials. A_s and A_f define the start and finish temperatures for free SME in the SMA, respectively. T_g is called the glass transition temperature and it defines the transition between glass and rubbery states for polymers. Shape changing and shape blocking are behaviours exhibited by SMP. Adapted from ref. **?**.

supplementary mechanism) shape blocking has been demonstrated by ref. **?** and **?**. While the former possesses reversible actuation and uses the buckling effect in a modified version of the kresling tower based structure, the latter is irreversible and uses a rigid mechanism to block its shape after being fully deployed.

Torsional SMA actuators are still a relatively emerging field and not much work has been done related to them. The main advantages of using torsional SMA actuators are their design simplicity, less space requirements and their ability to undergo large shear strains[?]. Ref. **?** fabricated and analytically studied a torsional SMA actuator which is embedded in origami structure and is responsible for folding the structure when heated. Torsional SMA actuated structures can be integrated with SMP to impart tunable stiffness to structures controlled by the temperature. Ref. **?** presents a weakly coupled FE model for a rigid host structure-SMA structure where first, a comparison between linear circular wire and torsional tubes is done based on FEA and then, their implementation on a morphing wing is presented. Although, a few works have been carried out to study the performance of millimeter-sized torsional SMA actuators using FEA, largely the works are based on the fabrication and realization of such folding structures. Moreover, works on FE studies having SMA actuators and host-structure/SMP coupling exist but are still less in number. This work contributes to the following:

1. Development of a FE based thermomechanical model which couples a torsional SMA actuator and a rigid hosting structure.
2. Influence of temperature-dependent tunable stiffness of SMPs for shape changing and shape blocking in torsional SMA actuated millimeter-sized origami robot applications.

In section 2, modelling is discussed laying out the conceptual and mathematical models, study cases and the constitutive behaviours of SMMs. Section 3 presents simulation results showing the influence of SMP stiffness for shape changing and shape blocking scenarios. Lastly, section 4 presents the outcome of the work and provides perspectives regarding the FEA based approach for designing of SMM based reconfigurable origami robots.

2. MODELLING

2.1 Conceptual Model

The complete structure is built as a millimeter-sized geometry (32 mm x 20 mm x 4 mm). Figure 2 shows the geometric model of the structure identifying the three material domains. The SMA actuator is represented by the 17 mm long cylinder in the middle having a diameter of 1 mm. The actuator is connected to the rigid structure on the ends of the cylinder. The rigid structure is built as a symmetric structure about the ZY plane with a distance of 10 mm between the two rigid parts. It consists of a connecting cubic block (3 x 6.5 x 3 mm) which connects the actuator to the main geometry having a cross section of 4 mm x 5 mm and a length of 32 mm. The rigid part is modelled with a very high stiffness. To have tunable stiffness, two SMP stripes are placed at the opposite ends of the structure. The thickness of each stripe is 1.5 mm while it is 0.4 mm in the middle to have a rotational hinge. Each SMP stripe is 4 mm wide.

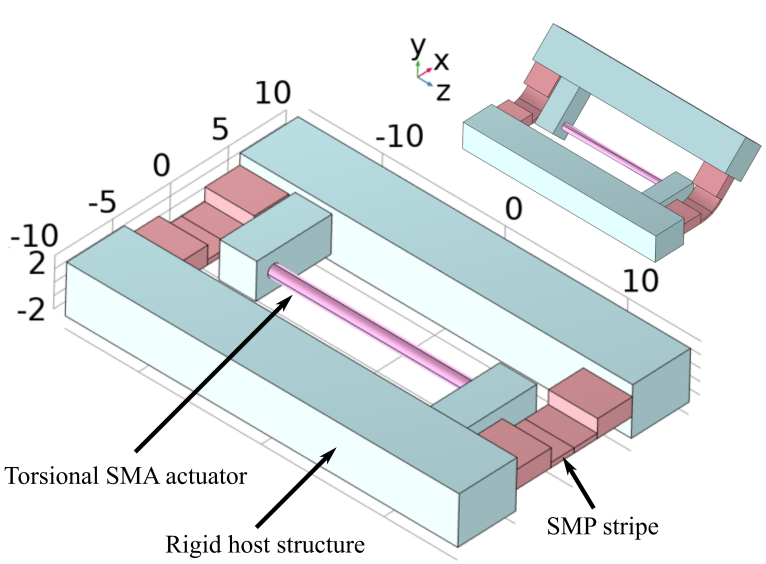

Figure 2: 3D geometry with different material domains. Small figure shows the folded geometry after pre strain (45). All dimensions are in *mm*.

2.2 Constitutive Behaviour

2.2.1 Shape Memory Alloy (SMA)

SMAs are alloys made of metals that are capable of undergoing large deformation without permanent change in shape thanks to their two distinct phases, martensite and austenite. Over the years, many efforts have been made to develop constitutive laws for SMAs[?]. These models can be mainly divided into 3 types which are the microscopic models, micro-macroscopic models and the phenomenological models[?]. The first two types provide more details than the third one but are complex to apply at device scale. Phenomenological models represent the average macroscopic behavior of SMAs. They take into account a limited number of internal variables and assume the material to be homogeneous which makes their implementation relatively easier. These models capture the behavior at macro and millimeter-sized level; therefore, they are a good choice for application level modelling. In the present work, 3D Lagoudas[?] constitutive phenomenological law has been used. In this law, to define the thermodynamic potential, the Gibbs free energy is used. It has the advantage of the custom definition of thermomechanical loading path for SMAs in the stress-temperature space. The internal variables that best represent the thermomechanical response of the SMAs at the micro-structure level are chosen. Thus, the constitutive model is represented by a set of internal state variables $(\sigma, T, \xi, \varepsilon^t)$, which represent the *stress*, the *temperature*, the *martensitic volume fraction* and the *transformation strain*, respectively. To precisely define the transformation between the two phases, a hardening function $f(\xi)$ is introduced. According to ref. **?**, this hardening function can be written in terms of the same state variable set and in different forms such as the

exponential form, cosine form, and polynomial form. Mathematically, the Gibbs free energy can be written as given in equation 1, where ρ is the *mass density*, $\mathcal{S}$ is the *effective compliance tensor*, α is the *effective thermal expansion coefficient*, c is the *effective specific heat*, s_0 is the *effective specific entropy* and u_0 is the *effective internal energy reference state*.

$$\mathrm{G}(\sigma, T, \xi, \varepsilon^t) = -\tfrac{1}{2\rho}\sigma : \mathcal{S} : \sigma - \tfrac{1}{\rho}\sigma : [\alpha\,(T - T_0) + \varepsilon^t] + c\left[(T - T_0) - T\ln\left(\tfrac{T}{T_0}\right)\right] - s_0 T + u_0 + \tfrac{1}{\rho} f(\xi) \tag{1}$$

Since the SMA has two distinct phases, martensite and austenite, its effective material properties are written in terms of the properties for the pure phases and martensitic volume fraction ξ, which can be written as:

$$\begin{gathered}\Upsilon(\xi) = \xi\Upsilon^M + (1-\xi)\Upsilon^A = \Upsilon^A + \xi\Delta\Upsilon \\ \Upsilon = \ \mathcal{S};\ \alpha;\ c;\ s_0;\ u_0\end{gathered} \tag{2}$$

where the superscripts A and M denote the austenitic and martensitic phases, respectively. The symbol Δ indicates the difference between the pure martensitic and austenitic phases. Using the Gibbs free energy formulation, the constitutive relation for the infinitesimal strain tensor can be written as:

$$\varepsilon = -\rho\frac{\partial G}{\partial \sigma} = \mathcal{S} : \sigma + \alpha\,(T - T_0) + \varepsilon^t \tag{3}$$

There is a key assumption in this model wherin the martensitic variant reorientation is not taken into account during the phase transformation and thus, any change in the current state of the material is directly linked to a change of the martensitic volume fraction ξ. Consequently, the evolution of transformation strain and the evolution of martensitic volume fraction can be related by the following equation:

$$\dot{\epsilon} = \Lambda\dot{\xi} \tag{4}$$

where Λ is the *normalized transformation tensor* that explains the direction of the martensitic transformation. It can be written as:

$$\Lambda = \begin{cases} \frac{3}{2}H\frac{\sigma'}{\bar{\sigma}'}; & \dot{\xi} > 0 \\ H\frac{\varepsilon^{t-r}}{\bar{\varepsilon}^{t-r}}; & \dot{\xi} < 0 \end{cases} \tag{5}$$

where H is a material parameter associated with the *maximum transformation strain*, $\sigma', \bar{\sigma}', \varepsilon^{t-r}, \bar{\varepsilon}^{t-r}$ are the *deviatoric stress tensor*, the *effective von Mises equivalent stress*, the *transformation strain tensor at the reversal point* and the *effective transformation strain at the reversal of the phase transformation*, respectively. The inequality of martensitic volume fraction rate $\dot{\xi}$ indicates the phase transformation direction. $\dot{\xi} > 0$, represents a forward phase transformation ($A \to M$), and vice versa.

For the present work, the mechanical, thermal and transformation properties are provided in table 1.

Table 1: Parameters for SMA model

Parameter	***Value***
Mechanical Properties	
E_A, E_M	75 GPa, 28 GPa
ν_A, ν_M	0.33, 0.33
Phase Properties	
M_s, M_f	325.15 K, 315.15 K
A_s, A_f	341.15 K, 351.15 K
C_A, C_M	7.4 MPa/K, 7.4MPa/K
Transformation Strain Properties	
ϵ_{trmax}	8%

2.2.2 Shape Memory Polymer (SMP)

SMPs are viscoelastic materials whose response varies over time even if applied load remains constant. Their properties depend on the frequency of loading and also on the temperature. The stiffness of SMP is generally increasing with frequency and decreasing with temperature (see figure 1).

The material used for this study has been already studied in ref. **?** in the frequency domain. In that work, using a DMA, experimental data was acquired (for a cylindrical specimen with a diameter of 1.75 mm and length of 6 mm) from 33 °C to 83 °C with an increment of 5 °C at a heating rate of 2 °C/min. This experimental data is used for the simulation reported in this work.

For the present work, the interest is to show the influence of the SMP stiffness according to the temperature on the motion range of an active hinge (shape changing) and also on the global rotational stiffness (shape blocking). Neglecting the dynamic experimental data, only the storage modulus $E^{'}$ at the minimum frequency (0.1 Hz) is extracted from the data and used as a function of temperature in this work. The storage modulus varies from 1455 MPa at 33 °C to 3.26 MPa at 83 °C. For the shape changing case, several values in between these two values are considered and a parametric study is performed. For the shape blocking study, only the the stiffness at 33 °C (1455 MPa) and 53 °C (18.2 MPa) is considered. The SMP is assumed as an isotropic linear elastic material with a constant elastic modulus in each study and a Poisson's ratio of 0.37.

2.3 Finite Element Model Configurations/Settings

Stationary analysis is performed neglecting the dynamic effects due to inertia. The domain mesh consists of mainly tetrahedra elements having quadratic shape functions, though other types of elements are also present but small in number. It is important to mention here that to achieve a large folding angle, the small strain assumption will not be valid in this study and large deformation theory (geometric nonlinearity) is used. With the SMA having a nonlinear constitutive behaviour and also the geometric nonlinearity, specific techniques are used to ensure convergence. A direct linear PARDISO solver is used along with nonlinear solver based on Newton Method. The technique of continuation method is used. It divides the total load/displacement in several steps thus making the load start from 0 and end at the desired final load. At each step, a study is performed and the initial guess is taken from the solution of the preceding step which ensures better convergence. To implement this, a continuation parameter (cont. para.) is used. The applied displacements/load and temperature (for SMA) are a function of this parameter. The solution is obtained at each parameter value. The continuation parameter is given as a number starting from 0 to a specific final value which is different in each of the two study cases.

2.4 Study Scenarios and Boundary Conditions

Two different studies are performed in order to represent the shape changing and shape blocking capabilities. Both studies are performed as a 3 step procedure.

In the first step (cont. para. = 0 - 1), the structure is loaded with an initial angular rotation of 45 on one side, while the other side of the structure is fixed. This is called as the 'Pre Strain' step. In the second step (cont. para. = 1 - 2), the structure is set free from the loaded side (while the other side is still fixed) and allowed to elastically release (called 'Elastic Release').

The aforementioned first two steps are common to both studies while the third step for each study is explained in subsequent subsections.

2.4.1 Case 1: Shape Changing

The main purpose of performing this study is to present shape changing/recovery (after an initial rotation) because of SME of the SMA actuator and also to see the influence of SMP stiffness on the motion and hence the final state of the structure.

After the two initial steps, in the third step (cont. para. = 2 - 4), the SMA is subjected to a temperature increase, thus activating the SME. The evolution of the thermal stimuli and applied displacements will be discussed in section 3.

Practically, this study represents the case when it is desired to achieve a partial or full unfolding/folding of the structure which can be controlled by controlling the temperature of the SMP.

2.4.2 Case 2: Shape Blocking

In real life, origami structures are light weight and soft. While it is not desired, a small disturbance can be enough to change their shape. SMP can be used in such scenarios to block the shape of the structure when desired. They can be cooled or left at room temperature to contribute to higher global stiffness and hence ensure the locking of the shape.

Following the step 2, in the third step (cont. para = 2 - 3), one side of the rigid part is subjected to a small normal force causing a very small rotation about the SMA axis, while the other side stays fixed. This study is performed to quantify the augmented rotational stiffness of the complete structure due to SMP for shape blocking application.

3. RESULTS AND DISCUSSION

3.1 Pre Strain

Figure 3 shows the spatial evolution of von Mises stress and the martensitic volume fraction ξ in the cross section of SMA actuator at the pre strained stage. As also observed by ref. **?**, because of the 45 rotation, the torsional SMA actuator undergoes large shear strains at the outer ends while it tends to zero at the center. This explains the increase of von Mises stress through the radial direction. Additionally, as the martensitic volume fraction is directly linked to the stress levels, the contours represent that there is more transformation at the ends and the martensitic volume fraction ξ is about 16%, while the austenite phase persists in the centre. In fact, even if the applied rotation tended to infinity, the volume fraction ξ would still not completely reach 100%.

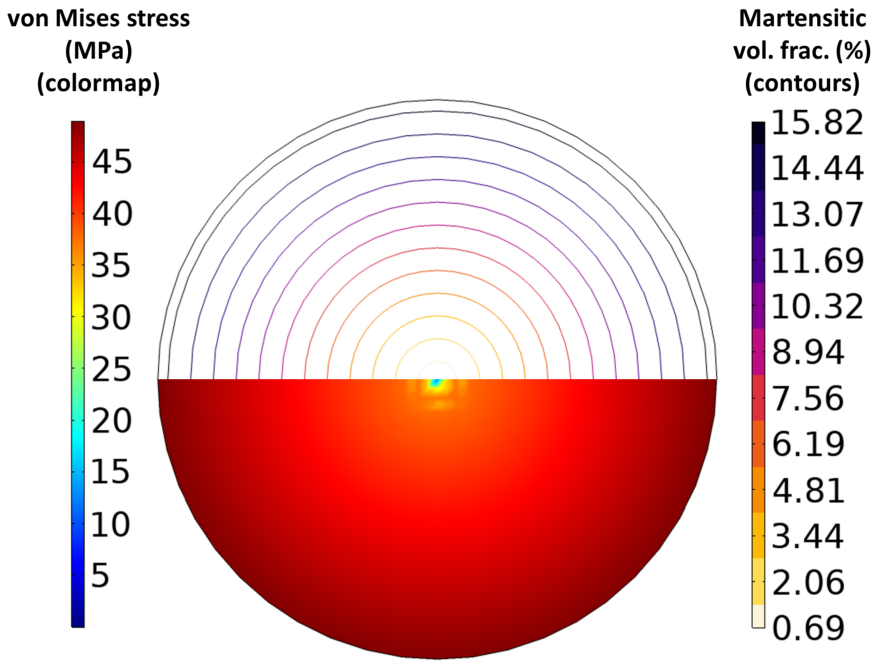

STRESS.png

Figure 3: Evolution of von Mises stress (colormap) and martensitic volume fraction 'ξ' (contours) in SMA cross section.

3.2 Shape Changing

3.2.1 Input parameters

Figure 4a shows the evolution of inputs during the three steps of the shape changing study. During the prestrain (cont. para. = 0 - 1), the structure is folded to an angle of 45, while it is fixed from the other end. This is

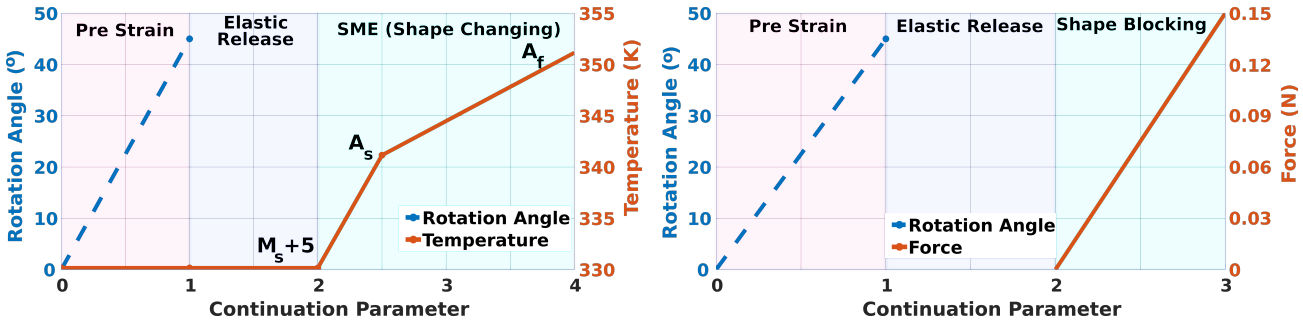

(a) **Case 1 - shape changing**: Evolution of applied rotation angle and temperature in SMA vs continuation parameter.

(b) **Case 2 - shape blocking**: Evolution of applied rotation angle and force vs continuation parameter. Temperature in SMA is constant at $(M_s + 5)$.

Figure 4: Input parameters for both studies.

followed by an elastic release (cont. para. = 1 - 2). In the shape changing step, (cont. para. = 2 - 4), the temperature of SMA increases from $M_s + 5$ to A_f at the end to demonstrate SME. As a result, the SMA actuator starts to experience reverse transformation from martensite to austenite, however the presence of SMP becomes a hindrance to that and depending on its stiffness, different final folding angles described as shape changing are achieved. This is further described in the subsequent subsections.

3.2.2 Influence of SMP Stiffness on Total Displacement

As a result of the SME of the SMA actuator, it is observed that the structure unfolds/deploys back to its initial unfolded state. However, this is the case only when there is no SMP patches. In the case when SMP patches are present, during reverse transformation, the structure faces some resistance depending on the stiffness of the SMP patches which limits the rotation angle travelled by the structure and thus, shape changing is achieved.

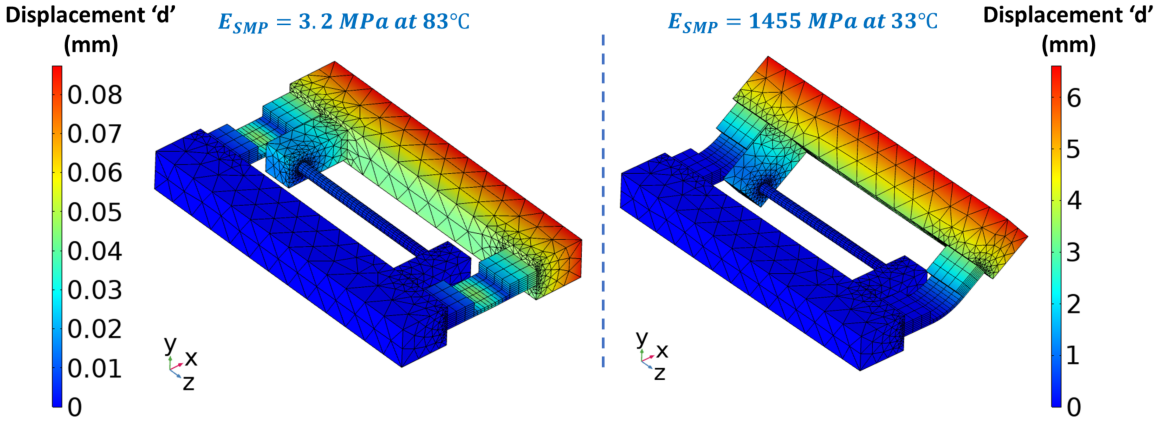

Figure 5: Influence of SMP modulus on shape changing after an initial rotation of 45. At low SMP stiffness (left), maximum shape changing from elastic release stage is observed ($d_{max} = 0.08$ mm), while at high modulus (right), just a slight restoration of rotation from elastic release stage is observed ($d_{max} = 6$ mm). The displacements shown here are relative to the unfolded initial state of the structure as shown in figure 2.

Figure 5 shows the total displacement of the structure at the final state of simulation (after the SME). The displacements shown are relative to the unfolded initial state of the structure as shown in figure 2. Two cases are shown. Both cases are achieved after a similar prestrain of 45 and elastic release. However, the two cases show the displacements for the two extreme cases of SMP stiffness. On the left, the case with the lowest SMP stiffness ($E_{SMP} = 3.2$ MPa) is shown, which occurs at a temperature of 83 °C, while shown on the right is

the case with the highest SMP stiffness (E_{SMP} = 1455 MPa), that occurs at a temperature of 33 °C. It is evident from the figure that at the final instance, for the lowest stiffness case (left), the structure nearly gets restored to its original unfolded state with a maximum displacement of just 0.08 mm. On the contrary, for the highest stiffness case (right), the SMA actuator faces a large resistance from the SMP during SME and ends up unfolding the structure by a very small angle as a result of which there is a total maximum displacement of 6 mm. Furthermore, it indicates that at ambient SMP temperature (high SMP stiffness), the SMP is able to block/limit the SME of the SMA.

For better quantification of the motion range, a parametric study was performed with 9 cases of SMP stiffness in between the two aforementioned extreme values.

3.2.3 Influence of SMP Stiffness on Rotation Angle: Parametric Results

Figure 6a represents the effect of SMP stiffness on the total angular rotation restored back by SME, as well as the percentage of shape changing (red text) in each case. The shown values of rotation angle are relative to the state of the structure after the elastic release. The percentage values are computed as the ratio of the achieved rotation angle and the initial prestrain angle of 45. The results represent an asymptotic trend with respect to the two extreme values. With an initial prestrain of 45 in all the cases, 99% shape changing is observed when the SMP offers very small stiffness, however, as the stiffness of SMP increases, the motion range of the structure becomes more limited and asymptotically reaches a minimal value of 7.1 resulting in just 16% shape changing. This demonstrates the capability of shape changing due to temperature-dependent tunable stiffness of the SMP material. By controlling the temperature, any desired angular rotation can be achieved within the bounds of the structure's maximum motion range.

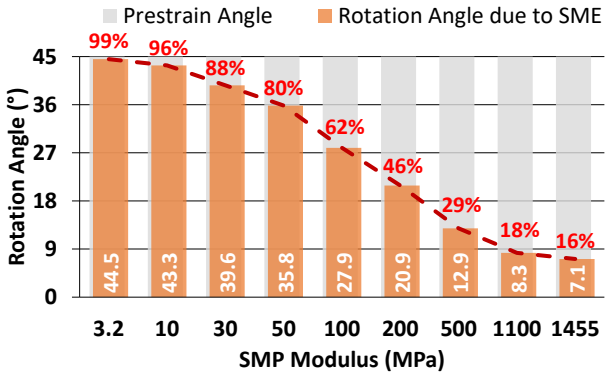

(a) Variation of rotation angle and shape changing percentage (red) after SME at different values of SMP modulus. A decreasing trend is observed with increasing stiffness.

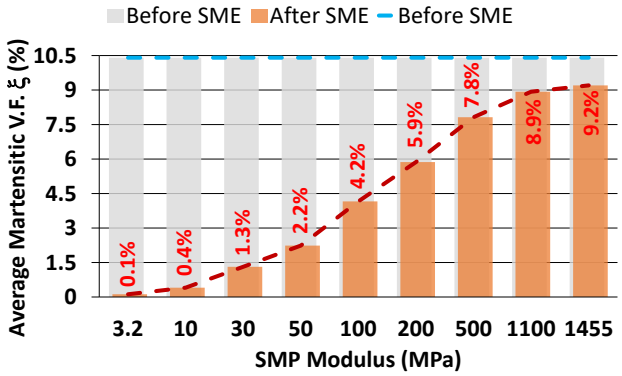

(b) Martensitic volume fraction ξ after SME at different values of SMP modulus. An increasing trend is seen with increasing stiffness.

Figure 6: Influence of SMP on rotation angle (6a) and martensitic volume fraction (6b).

3.2.4 Influence of SMP Stiffness on Average Martensitic Volume Fraction: Parametric Results

As the SMA actuator undergoes reverse transformation (SME), the volume fraction is bound to decrease, however, its final value depends on the strains at the final rotation angle with respect to the initial (prestrain) one. Figure 6b represents the average volume fraction of martensite ξ inside the SMA actuator at the final state (after SME). ξ, at the end of elastic release has a value of 10.4% which is shown by the blue straight dashed line. The orange columns represent the volume fraction (in %) at the final step for each case of SMP stiffness while the red dashed line represents the trend of the volume fraction. Similar to the case for rotation angle, an asymptotic trend is observed. For the case with the lowest SMP stiffness (E_{SMP} = 3.2 MPa), figure 6b shows that the martensitic volume fraction ξ is 0.1% which highlights that the SMA has gone through the reverse transformation almost completely. On the contrary, for the case with the highest SMP stiffness (E_{SMP} = 1455 MPa), the martensitic volume fraction is 9.2% which is very close to the initial value (10.4%, after elastic release), thus showing that there is very less reverse transformation.

Conclusively, it can be said that the motion range of the structure varies distinctively with the different values of SMP modulus and by controlling the temperature of the SMP stripes, shape changing can be achieved.

3.3 Shape Blocking

Another objective to have a SMA-SMP coupled model is the capability of resisting external disturbances from the environment. This can also be referred to as shape blocking. Since origami structures are light weight and soft, they have less inherent blocking abilities, it is therefore important to artificially enhance shape blocking abilities. In this section it is presented, that how by using some SMP patches, whenever desired, the rotational stiffness of the structure can be enhanced.

3.3.1 Input Parameters

Figure 4b presents an evolution of inputs for the three steps of the shape blocking study with the continuation parameter. The first two steps are the same as in the case of shape changing and after the elastic release, while in the third step (cont. para. = 2 - 3), a force of 0.15 N is exerted on one edge resulting in a small angular rotation towards the initial unfolded state.

3.3.2 Rotational Stiffness

This section provides the quantification of the rotational stiffness offered by the folded structure in resistance to an external load. The objective is to enhance the shape blocking capabilities, not shape changing. For this, SME should not be activated (because it helps in shape changing), therefore the temperature in the SMA during this study is constant. It is important to mention here that since the SMP material will intuitively provide more stiffness at lower temperatures and will offer less stiffness at higher temperatures (higher than its glass transition temperature), so only three cases are considered: first without SMP, second with normal SMP (33 °C, $E_{SMP} = 1455$ MPa), and third with hot SMP (53 °C, $E_{SMP} = 18.2$ MPa).

Figure 7 presents the linear evolution of reaction torque vs rotation angle for the complete structure caused as a result of the applied force for the three cases. The red line represents the case when no SMP material is used whereas the blue and yellow lines show the cases when two stripes of SMP material are used at low/normal (33 °C) and high (53 °C) temperatures respectively. The initial value of the rotation angle is taken from the end of elastic release stage and starts from 0. The reaction torque is computed about the center of the structure (in the middle of the SMA axis). The markers on the figure correspond to the results at each continuation parameter. Initially, there is no rotation and no resulting reaction torque.

For the applied load, in the case without the SMP, the structure rotates approx. 0.75 and generates a reaction torque of approx. 1.5 N.mm which results in a rotational stiffness (slope of red curve) of $K_\theta \approx 1.97$ N.mm/°. For the case with the (normal) SMP at 33 °C, the structure rotates approx. 0.6 and generates a reaction torque of approx. 1.5 N.mm which results in a rotational stiffness (slope of blue curve) of $K_\theta \approx 2.5$ N.mm/°. Lastly, for the case with (hot) SMP at 53 °C, the rotational stiffness (slope of yellow curve) is $K_\theta \approx 2$ N.mm/°, which is almost the same as in the case without the SMP (1.97 N.mm/°).

Conclusively, it can be deduced that because of the use of SMP material (at low temperature (33 °C)), the rotational stiffness of the structure increases by approximately 25% as compared to the 'without SMP' case, thus resulting in enhanced shape blocking (higher resistance to external disturbances). However, when the SMP is at a high temperature (53 °C), the increase in the global rotational stiffness is negligible and thus, it becomes favorable to change the shape.

Furthermore, increasing the thickness and width of the SMP stripes increases the rotational stiffness significantly and a parametric study can be performed to quantify this increase in the global rotational stiffness.

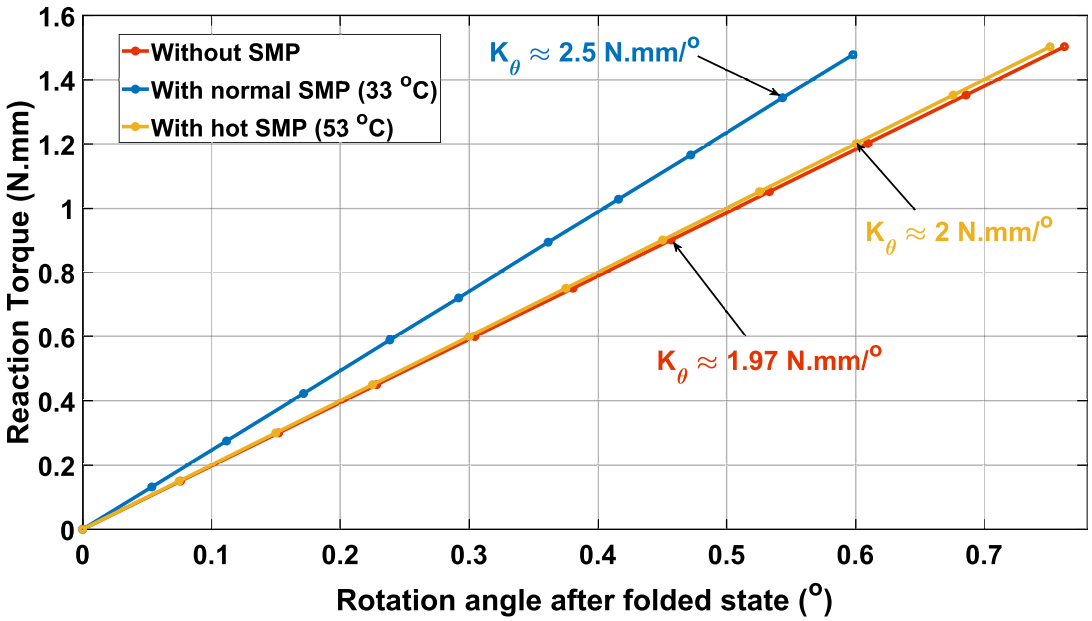

Figure 7: Variation of rotation angle after elastic release state vs reaction torque about SMA axis. The red curve shows the case without SMP, the blue curve shows the case with the normal SMP ($E_{SMP} = 1455$ MPa) and the yellow curve shows the case with the hot SMP ($E_{SMP} = 18.2$ MPa). An increase of 25% in the rotational stiffness is observed by using the SMP at low temperature, while, with the SMP at high temperature, the increase in stiffness is negligible. K_θ represents the rotational stiffness.

4. CONCLUSIONS AND PERSPECTIVES

The objective of this work was to build and simulate a strongly coupled shape memory material based self deploying thermomechanical model of an origami hinge, capable of both, shape changing and shape blocking. A torsional SMA actuator mounted on a rigid structure with patches of SMP material was presented. The SMA was represented by the 3D Lagoudas constitutive law and the SMP was assumed as a linear isotropic material. The technique of continuation method was implemented along with a nonlinear solver to resolve a model consisting of nonlinear constitutive behaviour and geometric nonlinearity. While the SMA actuator imparts the capability of self deployment because of the SME, the SMP (thanks to its temperature-dependent tunable stiffness) provides the advantage of controlling the unfolding angle (shape changing) and enhancing the ability to block the shape when desired.

For the given geometric configuration, two study cases were presented namely, the shape changing and shape blocking. For shape changing, it was concluded that the folding of the structure can be controlled and can undergo a percentage shape changing from 16% to 99% thanks to the tunable stiffness of SMP. For shape blocking, it was deduced that by using SMP at a lower temperature (33 °C), the global rotational stiffness can be increased by approximately 25%, therefore enhancing the shape blocking capabilities. However, when the SMP is heated and used at a higher temperature (53 °C), there is a very small added stiffness and it becomes favorable to fold/unfold the structure (change the shape).

Furthermore, as a future perspective, the geometry can be topologically optimized to obtain the desired shape changing and shape blocking properties. Naturally, the proposed hinge will be integrated on a physical prototype for experimental validation and performance assessment.

ACKNOWLEDGMENTS

This work was supported by the French National Agency for Research (OrigaBot ANR-18-CE33-0008), and EUR EIPHI (Contract No. ANR-17-EURE-0002).